HHS Public Access

Author manuscript

J Mater Chem B Mater Biol Med. Author manuscript; available in PMC 2015 August 31.

Published in final edited form as:

J Mater Chem B Mater Biol Med. 2015 April 14; 3(14): 2816–2825. doi:10.1039/C4TB02042A.

Enhancing the protein resistance of silicone via surface-restructuring PEO-silane amphiphiles with variable PEO length

M. A. Rufin[a], **J. A. Gruetzner**[a], **M. J. Hurley**[a], **M. L. Hawkins**[a], **E. S. Raymond**[b], **J. E. Raymond**[c], and **M. A. Grunlan**[a,d]

M. A. Grunlan: mgrunlan@tamu.edu

[a]Department of Biomedical Engineering, Texas A&M University, College Station, TX 77843-3120

[b]Department of Neuroscience and Experimental Therapeutics, Texas A&M University, College Station, TX 77843-3120

[c]Department of Chemistry, Texas A&M University, College Station, TX 77843-3120

[d]Department of Materials Science and Engineering, Texas A&M University, College Station, TX 77843-3120

Abstract

Silicones with superior protein resistance were produced by bulk-modification with poly(ethylene oxide) (PEO)-silane amphiphiles that demonstrated a higher capacity to restructure to the surface-water interface versus conventional non-amphiphilic PEO-silanes. The PEO-silane amphiphiles were prepared with a single siloxane tether length but variable PEO segment lengths: α-$(EtO)_3Si(CH_2)_2$-oligodimethylsiloxane$_{13}$-*block*-poly(ethylene oxide)$_n$-OCH_3 (n = 3, 8, and 16). Conventional PEO-silane analogues (n = 3, 8 and 16) as well as a siloxane tether-silane (i.e. no PEO segment) were prepared as controls. When surface-grafted onto silicon wafer, PEO-silane amphiphiles produced surfaces that were more hydrophobic and thus more adherent towards fibrinogen versus the corresponding PEO-silane. However, when blended into a silicone, PEO-silane amphiphiles exhibited rapid restructuring to the surface-water interface and excellent protein resistance whereas the PEO-silanes did not. Silicones modified with PEO-silane amphiphiles of PEO segment lengths n = 8 and 16 achieved the highest protein resistance.

Introduction

Silicones, particularly silica-reinforced, crosslinked poly-dimethylsiloxane (PDMS), are widely used for medical, marine and industrial applications. These include blood-contacting devices (e.g. hemodialysis catheters, catheter balloons and cardiac pacing leads)[1-3] and marine coatings.[4] Unfortunately, as a result of their extreme hydrophobicity, the performance of silicones is severely limited by poor resistance to biomolecules such as proteins.[5, 6] For example, in the case of blood-contacting devices, the non-specific

Correspondence to: M. A. Grunlan, mgrunlan@tamu.edu.

Electronic Supplementary Information (ESI) available: [Contact angle analysis data for surface-grafted wafers (Table S1), contact angle analysis data for bulk-modified silicones (Table S2), and protein adsorption fluorescent intensity measurements for bulk-modified silicones (Table S3)].

adsorption of plasma proteins is considered the first step of thrombosis and even infection.[7-9] Various modifications have been utilized to hydrophilize silicones in order to reduce protein adsorption, including physical, chemical and combined approaches.[10-14]

Silicone modification with poly(ethylene oxide) (PEO; or poly(ethylene glycol) (PEG)) represents arguably the most widely utilized method for enhancing hydrophilicity and protein resistance.[15-19] The exceptional protein resistance of PEO is attributed to its hydrophilicity and hydration, as well as its configurational mobility.[20-23] The biocompatibility[24] and recently demonstrated *in vivo* oxidative stability[25] of PEO contributes to its widespread use. Notably, the protein resistance of PEO has largely been assessed for chains surface-grafted onto physically stable substrates such as gold,[26-28] silicon[29-31] and glass.[32, 33] For these "model PEO surfaces," PEO chains are maintained at the surface irrespective of the environment (i.e. air versus water). In contrast, PEO chains incorporated into silicones are subject to surface reorganization upon exposure to a different environment.[34] This process has been studied mainly in terms of hydrophobic recovery (i.e. loss of hydrophilicity with exposure to air) such as that observed for plasma treated silicones.[35] This behavior is attributed to the low surface energy of silicones,[36, 37] coupled with their high chain flexibility.[38, 39] For example, hydrophobic recovery has been observed for PEO-modified silicones formed by bulk crosslinking with triethoxysilylpropyl PEO monomethyl ether [$(EtO)_3Si(CH_2)_3$-$(OCH_2CH_2)_x$-OCH_3][40, 41] as well as allyl PEO monomethyl ether (CH_2=$CHCH_2$-$(OCH_2CH_2)_x$-OCH_3.[42] Hydrophobic recovery is also observed for surface-grafted PEO chains such as those prepared with allyl PEO monomethyl ether.[42, 43] However, since biofouling events such as protein adsorption occur in an aqueous environment, the rapid and substantial surface restructuring of PEO to the surface-water interface is of critical importance.

Towards the goal of enhancing the protein resistance of silicones, we sought to improve the capacity of PEO to migrate to the surface-water interface by altering its molecular structure. Previously, we reported PEO-silane amphiphiles prepared with a siloxane tether of varying lengths (*m*) separating the PEO segment from the crosslinkable ethoxy silane groups [$\alpha(EtO)_3Si(CH_2)_2$-oligodimethylsiloxane$_m$-$(OCH_2CH_2)_8$-OCH_3; m = 0, 4, 13].[44] The siloxane tether distinguishes the PEO-silane amphiphiles from the analogous conventional PEO-silanes noted above which contain a short alkane (e.g. propyl) spacer.[40-43] The siloxane tether is characterized by high flexibility resulting from the wide bond angle (∼145 °) and low barrier to linearization (∼0.3 kcal/mol) of Si-O-Si dimethylsiloxane bonds, features that give rise to low glass transition temperatures (e.g. PDMS, T_g = -125 °C).[38, 39] Like a silicone elastomer, the siloxane tether is also hydrophobic, imparting an amphiphilic character to these PEO-silanes. We anticipated that the flexibility and similarly hydrophobic nature of the siloxane tether would facilitate water-driven migration to the surface of a bulk-modified silicone thereby reducing protein adsorption. Indeed, when the PEO-silane amphiphiles (m = 0, 4, 13) were bulk crosslinked with α,ω-bis(Si-OH) PDMS (M_n = 3000 g/mol), protein resistance[44] as well as bacteria and diatom resistance[45] increased with siloxane tether length. Furthermore, extensive atomic force microscopy (AFM) analysis has confirmed the water-driven migration of PEO to these silicone coating surfaces to form nanocomplex surfaces.[46] Herein, we evaluated the impact of PEO segment length by bulk

crosslinking a medical grade RTV silicone with three PEO-silane amphiphiles of different PEO segment lengths (n = 3, 8 and 16) and a single siloxane tether length (m = 13) (Figure 1). Given the protein resistance of PEO oligomers when surface-grafted onto a model substrate,[26] PEO-silane amphiphile (n = 8) was selected for our previous work to enhance the protein resistance of bulk-modified silicones.[44, 46-49] Thus, for this study, values of "n" (3, 8, and 16) were chosen as they are "substantially" different from one another (by a factor of approximately two) and thus were predicted to have different restructuring potentials. Analogous conventional PEO-silanes or "PEO-controls" (i.e. no siloxane tether, n = 3, 8, and 16) as well as a "siloxane-control" (i.e. no PEO segment, m = 13) were likewise evaluated to highlight the effect of the siloxane tether. Water-driven surface restructuring was quantified by temporal static contact angle analysis of water droplets, and resistance to fibrinogen was also measured. In addition, PEO-silane amphiphiles, PEO-controls and the siloxane-control were each surface-grafted onto silicon wafers in order to evaluate their protein resistance in the absence of surface restructuring. This study therefore represents an effort to better understand the influence of the siloxane tether and PEO segment length on the protein resistance and surface restructuring of PEO-silanes through systematic comparisons versus controls.

Results and discussion

Surface-grafted coatings on silicon wafers

The protein resistance of PEO-silane amphiphiles (n = 3, 8, and 16) in the absence of water-driven restructuring to the surface was evaluated with surface-grafted coatings prepared on silicon wafers. PEO-controls (n = 3, 8, and 16) and the siloxane-control were likewise evaluated to elucidate the impact of the siloxane tether.

X-ray photoelectron spectroscopy (XPS)—The surface-grafting of conventional PEO-silanes onto silicon wafers has been widely reported.[29-31] Likewise, the successful surface-grafting of PEO-silane amphiphiles (n = 3, 8, and 16) was confirmed via XPS with the PEO-control (n = 8) and siloxane-control serving as controls. Surface elemental atomic percent compositions are reported in Table 1. For the oxidized silicon wafer, the O 1s and Si 2p peaks correspond to the wafer composition whereas the carbon (C 1s) is attributed to adsorbed contaminants.[50, 51] Following surface-grafting, a decrease in Si 2p and increase in C 1s content was observed as expected. To further confirm surface-grafting, the C 1s peak was deconvoluted into two peaks of different binding energies and normalized to the peak centered at 284.5 eV (Figure 2). These peaks correspond to the C-C/C-Si (at 284.5 eV) and C-O (at 286.4 eV) of PEO.[43] The areas of the C-C/C-Si and C-O peaks are reported in Table 1. When surfaces were grafted with PEO-silane amphiphiles, C-O content increased with PEO-segment length (n) and a concomitant decrease in C-C/C-Si content was also observed. As expected, the relative quantity of C-O on the surface grafted with the PEO-control was greatest due to the absence of C-Si associated with the siloxane tether that was present on all other samples. Finally, for the surface-grafted siloxane-control, C-O content was very low and may be attributed to residual unreacted ethoxy groups. Together, these results confirm the successful grafting of PEO-silane amphiphiles to silicon wafers.

Ellipsometry—As chain spacing is known to influence protein resistance of grafted PEO coatings,[52, 53] it was important to ensure that the graft density was similar for all samples using ellipsometry. Dry thickness values (*h*) of grafted PEO-silane amphiphiles, PEO-controls, and the siloxane-control were measured and the obtained values of *h* were then used to estimate the chain density (σ) (Table 2):[54-56]

$$\sigma=(h\rho N_A)/M_n \quad (1)$$

where ρ is the density of the dry grafted layer, N_A is Avogadro's number and M_n is the number average molecular weight of the chain. The chain distance or "spacing" (*D*, nm) (i.e. distance between grafting sites) was also calculated (Table 2):[56]

$$D=(4/\pi\sigma)^{1/2} \quad (2)$$

Utilizing the described grafting conditions, all grafted layers were found to have similar chain spacing (*D*) (1.0 - 1.5 nm) except for the PEO-control (*n* = 8). This particular composition yielded high values of *h* (~4.3 nm) which are significantly higher than the fully extended chain length of the PEO segment (~ 2.8 nm),[57] indicative of substantial multilayer formation. To prevent multilayer formation and increase *D*, the grafting conditions for the PEO-control (*n* = 8) were adjusted as follows: grafting solution concentration = 0.006 M, exclusion of water droplet from grafting solution, and cure under vacuum at RT.

For all compositions of surface-grafted chains to be in the brush regime, *D* must be less than twice the Flory radius ($2R_f$).[53] For each chain composition, R_f was calculated on the basis of the length of one monomer (*a*) and the degree of polymerization (*N*) as follows: [53, 58, 59] (i) for the siloxane-control in a poor solvent (water): $R_f = aN^{1/3}$, where *a* = 0.5 nm and *N* = 13 and (ii) for the PEO-controls in a good solvent (water): $R_f = aN^{3/5}$, where *a* = 0.35 nm and *N* = *n*. For all of these controls, $D < 2R_f$. Calculation of R_f for the PEO-silane amphiphiles is complicated by the fact that these contain two "blocks" (i.e. siloxane tether and PEO segment) of differing solubility in water. Thus, R_f was individually calculated on the basis of both the siloxane tether and the PEO segment[47] using the aforementioned equations. For all grafted PEO-silane amphiphiles, $D < 2R_f$, even when considering the lower of the two calculated R_f values. Thus, for all grafted chains, a brush regime was obtained.

Water contact angle analysis—An oxidized silicon wafer provides a physically stable surface such that the concentration of grafted chains is maintained at the surface, irrespective of an air or water environment. Thus, the impact of PEO-silane amphiphile structure, including PEO segment length, on surface wettability (i.e. θ_{static}) may be elucidated by comparing these grafted surfaces to those prepared with the PEO-controls and the siloxane-control. θ_{static} was measured immediately after water droplet deposition (0 sec) and at 2 min (Figure 3; Table S1). For all grafted surfaces, θ_{static} (0 s) was very similar to θ_{static} (2 min) due to the expected lack of surface restructuring. For the siloxane-control grafted surface, the hydrophobicity of the siloxane tether (and the absence of a hydrophilic PEO segment) led to a hydrophobic surface as characterized by $\theta_{static} > 90°$.[60] In the case of PEO-control grafted surfaces, surface hydrophilicity increased (i.e. θ_{static} decreased) with

increased PEO-segment length (*n*). This trend was likewise observed for PEO-silane amphiphile grafted surfaces. However, due to the contributions of the PEO-silane amphiphiles' hydrophobic siloxane tethers, these surfaces were substantially more hydrophobic versus the corresponding PEO-controls (i.e. same *n*).

Protein adsorption—Human fibrinogen (HF) was chosen as the protein for these adsorption studies due to its well-established influence in surface-induced thrombosis by causing platelet adhesion and activation.[61-66] Its use in evaluating the thromboresistance of materials *in vitro* has also been well established.[26, 40, 46-49, 53, 54, 63, 67-71] Adsorption of HF onto surface-grafted silicon wafers was measured by quartz crystal microbalance with dissipation monitoring (QCM-D) (Figure 4). QCM-D has been widely used for measuring adsorption of proteins on low-fouling grafted monolayers and thin films.[70, 72-74] The Sauerbrey model was used to approximate the mass of fibrinogen due to the relatively low dissipation of the adsorbed protein.[68] Furthermore, the changes in frequency and dissipation for the most protein-resistant surfaces were too small for the software to accurately calculate the mass using a viscoelastic (Voigt) model. Mass was calculated from the seventh overtone of frequency.

Proteins, including HF, are known to adsorb more onto hydrophobic versus hydrophilic surfaces.[75, 76] Indeed, the degree of hydrophobicity of the grafted surfaces (as indicated by θ_{static} reported in Figure 3) correlates well with the observed amounts of HF adsorbed (Figure 4). For instance, the siloxane-control produced the most hydrophobic grafted surface which led to the highest level of HF adsorption. Due to increasing hydrophilicity, the protein resistance of grafted surfaces with PEO-silane amphiphiles as well as PEO-controls increased with PEO-segment length (*n*). Notably, for a given PEO-segment length (*n*), the PEO-silane amphiphile adsorbed more HF than the PEO-control which is consistent with the higher hydrophobicity of the former. These results agree with the exceptionally low fouling nature observed for PEO chains grafted onto stable surfaces.[26, 28-30, 32, 33]

Bulk-modified silicone coatings

In order to evaluate the capacity of the silanes to undergo water-driven surface reorganization and reduce protein adsorption, a medical-grade RTV silicone was bulk-modified with PEO-silane amphiphiles (*n* = 3, 8, and 16), PEO-controls (*n* = 3, 8, and 16) and the siloxane-control. Each silane was introduced at a constant level (0.05 mmol of silane per 1.0 g silicone) and the solvent-cast films were cured on glass slides (Figure 5). The thicknesses of all films were measured by an electronic caliper and found to be 0.14 ± 0.01 mm. When modified with the hydrophobic siloxane-control, the coating appearance resembled that of the unmodified silicone. The lack of increased opacity of these films was attributed to the solubility of the siloxane-control in the silicone matrix. In contrast, silicones modified with PEO-controls were substantially more opaque and notably so when compared to those prepared with the corresponding PEO-silane amphiphiles. Opacity increased, particularly for the PEO-controls, as the PEO-segment length (*n*) increased. The lesser increase in opacity of silicones modified with PEO-silane amphiphiles may be attributed to reduced phase separation stemming from the solubility of the hydrophobic siloxane tether in the silicone matrix.

Water contact angle analysis—As noted, AFM was previously used to confirm the water-driven formation of a PEO-enriched surface for silicone modified with the PEO-silane amphiphile (n = 8).[46] Water-driven surface restructuring of bulk-modified silicones was evaluated by temporally measuring θ_{static} of a water droplet placed on the surface over a 3 min period (Figure 6, Table S2). As expected, the unmodified silicone was very hydrophobic and the θ_{static} value did not change significantly during the 3 min measurement. The siloxane-control produced a modified silicone that was also very hydrophobic but displayed a slight decrease in θ_{static} over 3 min ($\Delta = \sim 12°$). However, at 3 min, θ_{static} was still > 90° and therefore hydrophobic.[60] Notably, silicones modified with PEO-controls also remained hydrophobic after 3 min ($\theta_{static,\ 3\text{-}min} > 90°$), similarly exhibiting only a moderate decrease in θ_{static} 3 min after droplet deposition (n = 3, $\Delta = \sim 19°$; n = 8, $\Delta = \sim 15°$; n = 16, $\Delta = \sim 12°$). Thus, the PEO-controls demonstrated a limited capacity to migrate to the surface-water interface and hydrophobicity was only slightly diminished with decreased PEO length. In contrast, when modified with PEO-silane amphiphiles, silicone surfaces underwent extensive and rapid water-driven surface reorganization as noted by large decreases in θ_{static} over a 3 min period (n = 3, $\Delta = \sim 33°$; n = 8, $\Delta = \sim 88°$; n = 16, $\Delta = \sim 59°$). Thus, the siloxane tether critically facilitates the migration of PEO segments to the surface-water interface. Due to this enhanced surface reorganization, initially hydrophobic surfaces quickly became more hydrophilic, with hydrophilicity increasing in the order: n = 3 ($\theta_{static,\ 3\text{-}min} = \sim 84°$) < n = 16 ($\theta_{static,\ 3\text{-}min} = \sim 57°$) < n = 8 ($\theta_{static,\ 3\text{-}min} = \sim 29°$). Thus, the PEO segment length of PEO-silane amphiphiles produced an obvious impact. For n = 8, modified silicones displayed the greatest decrease in θ_{static} over 3 min (i.e. Δ) and also achieved the highest hydrophilicity (i.e. $\theta_{static,\ 3\text{-}min}$). For n = 16, the longer PEO segment length likely imparts a greater steric challenge for water-driven surface reorganization. In contrast, for n = 3, while short PEO segments may more readily move to the surface-water interface, the reduced number of PEO repeating units diminishes the relative potential to increase hydrophilicity.

Protein adsorption—Protein resistance of the bulk-modified silicone “thick” films was determined via confocal microscopy.[44, 46, 48, 49] Adsorption of fluorescently-labeled HF (100 μg/mL) was measured on silicone in terms of absolute fluorescent intensity (Table S3) and that normalized to unmodified silicone (Figure 7). The unmodified silicone, due to its high hydrophobicity, resulted in characteristically high protein adsorption. Due to its hydrophobic nature, the siloxane-tether produced modified silicones with similarly high protein adsorption. Despite modification of silicones with PEO-controls (n = 3, 8, and 16), protein adsorption was also high. This is notably contrary to the high protein repellency of PEO-controls when grafted onto silicon wafers (Figure 4). This can be explained by the contact angle analysis that demonstrates that the PEO segments comprising the PEO-controls are severely inhibited in their migration to the surface-water interface where protein adsorption occurs (Figure 6). The PEO-silane amphiphile (n = 3), due to its short PEO segment length and corresponding inability to effectively hydrophilize the surface-water interface (Figure 6), also produced modified silicones that adsorbed high levels of protein. However, distinctively low protein adsorption was observed for silicones modified with PEO-silane amphiphiles (n = 8 and n = 16), with the PEO-silane amphiphile (n = 8) yielding the lowest of the two. This agrees with the contact angle analysis that shows the rapid

transition from a hydrophobic to hydrophilic surface, indicative of highly efficient water-driven PEO surface migration (Figure 6). Thus, while these PEO-silane amphiphiles demonstrated reduced protein repellency versus the corresponding PEO-controls when surface-grafted onto silicon wafers (Figure 4), they are superior and highly effective in reducing protein adsorption onto bulk-modified silicones.

Experimental

Materials

Vinyltriethoxysilane (VTEOS), triethoxysilane, α,ω-bis-(SiH)oligodimethylsiloxane [M_n = 1000 – 1100 g/mol per manufacturer's specifications; M_n = 1096 g/mol per ^{1}H NMR end group analysis; ^{1}H NMR (δ, ppm): 0.05 – 0.10 (m, 78H, SiC*H*$_3$), 0.185 (d, *J* = 2.7 Hz, 12H, SiC*H*$_3$) and 4.67 – 4.73 (m, 2H, Si*H*)] and allyl methyl PEO$_3$[M_n = 204 g/mol per manufacturer's specifications; M_n = 204 g/mol per ^{1}H NMR end group analysis; ^{1}H NMR (δ, ppm): 3.35 (s, 3H, OC*H*$_3$), 3.50 – 3.67 (m, 12H, OC*H*$_2$C*H*$_2$), 4.00 (dt, *J* = 6.0 and 1.5 Hz, 2H, CH$_2$=CHC*H*$_2$O), 5.13 – 5.28 (m, 2H, C*H*$_2$=CHCH$_2$O), 5.82 – 5.96 (m, 1H, CH$_2$=C*H*CH$_2$O)] were purchased from Gelest. Allyl methyl PEO [Polyglykol AM 450, M_n = 292 – 644 g/mol per manufacturer's specifications; M_n = 424 g/mol per ^{1}H NMR end group analysis; ^{1}H NMR (δ, ppm): 3.35 (s, 3H, OC*H*$_3$), 3.51 – 3.66 (m, 32H, OC*H*$_2$C*H*$_2$), 4.00 (d, *J* = 5.4 Hz, 2H, CH$_2$=CHC*H*$_2$O), 5.13 – 5.28 (m, 2H, C*H*$_2$=CHCH$_2$O), 5.82 – 5.96 (m, 1H, CH$_2$=C*H*CH$_2$O)] was graciously provided by Clariant. Anhydrous magnesium sulfate ($MgSO_4$), hydrogen peroxide (H_2O_2) solution (30%) and glass microscope slides (75 mm × 25 mm × 1 mm), and phosphate buffer solution (PBS, without calcium and magnesium, pH = 7.4) were purchased from Fisher. Sulfuric acid (H_2SO_4, 95–98%), PEO mono methyl ether [M_n = 750 g/mol per manufacturer's specifications, M_n = 736 g/mol per ^{1}H NMR end group analysis; ^{1}H NMR (δ, ppm): 3.37 (s, 3H, OC*H*$_3$) and 3.53 – 3.73 (m, 64H, OC*H*$_2$C*H*$_2$)], sodium hydride (NaH; 60 wt% dispersion in mineral oil), allyl bromide, RhCl(Ph$_3$P)$_3$ (Wilkinson's catalyst), Pt-divinyltetramethyl-disiloxane complex (Karstedt's catalyst), and human fibrinogen (HF; M_w = 340 kDa; lyophilized powder; ≥90% clottable protein) were purchased from Sigma-Aldrich and were used as received. Organic solvents were also purchased from Sigma-Aldrich and were dried over 4 Å molecular sieves prior to use. Silicon wafers (111) were obtained from University Wafer, Inc. Silica-coated QCM-D sensor crystals (QSX-303) were purchased from Q-Sense. Medical-grade RTV silicone (MED-1137) was purchased from NuSil. Per manufacturer specifications, MED-1137 is comprised of α,ω-bis(Si–OH)PDMS, silica (11–21%), methyltriacetoxysilane (<5%), ethyltriacetoxysilane (<5%), and trace amounts of acetic acid. The Alexa Fluor 546-dye conjugate of HF (AF-546 HF; M_w = 340 kDa; lyophilized) was obtained from Invitrogen.

Synthetic approach

All reactions were run under a N_2 atmosphere with a Teflon-covered stir bar to agitate the reaction mixture. Chemical structures were confirmed with nuclear magnetic resonance (NMR) spectroscopy using a Mercury 300 MHz spectrometer operating in the Fourier transform mode and with $CDCl_3$ as the standard.

Synthesis of allyl methyl PEO_{16}—Allyl methyl PEO_{16} was prepared using a procedure adapted from literature.[77, 78] PEO methyl ether (M_n 736 g/mol, 13.98 g, 19 mmol) was dissolved in 90 mL tetrahydrofuran (THF) and added dropwise to a chilled (0 °C) NaH dispersion (6.24 g, 156 mmol) in 120 mL THF. The reaction was then warmed to room temperature (RT) and stirred for 6 h. Next, the PEO solution was chilled, allyl bromide (19.32 g, 160 mmol) in 120 mL THF was added dropwise, and the mixture was warmed to RT and stirred for 16 h. The reaction was then filtered to remove precipitates and volatiles removed under reduced pressure. The resulting orange oil was dissolved in 75 mL de-ionized (DI) water and washed 3 times with 75 mL toluene. The product was extracted 3 times with 50 mL chloroform. The chloroform solution was then dried with anhydrous $MgSO_4$, filtered, and volatiles removed under reduced pressure to yield the final product (8.32 g, 56 % yield) as a white, waxy solid. ^{1}H NMR (δ, ppm): 3.36 (s, 3H, OCH_3), 3.51 – 3.68 (m, 64H, OCH_2CH_2), 4.00 (dt, J = 5.7 and 1.5 Hz, 2H, CH_2=$CHCH_2O$), 5.14 – 5.28 (m, 2H, CH_2=$CHCH_2O$), 5.83 – 5.96 (m, 1H, CH_2=$CHCH_2O$).

Synthesis of PEO-silane amphiphiles (*n* = 3, 8, and 16)—PEO-silane amphiphiles (Figure 1) were prepared as previously reported for n = 8.[44] Wilkinson's-catalyzed regioselective hydrosilylation of VTEOS and α,ω-bis-(SiH)oligodimethyl-siloxane$_{13}$ produced "***1***" which was then subjected to Karstedt's-catalyzed hydrosilylation with the designated allyl methyl PEO_n.

PEO-silane amphiphile (n = 3): *1* (22.11 g, 17.2 mmol), allyl methyl PEO_3 (3.50 g, 17.2 mmol) and Karstedt's catalyst were reacted together. In this way, the product (25.76 g, 94% yield) was obtained. ^{1}H NMR (δ, ppm): 0.00 – 0.15 (m, 90H, $SiCH_3$), 0.48 – 0.55 (m, 2H, $SiCH_2CH_2CH_2$), 0.56 (s, 3H, $SiCH_2CH_2$), 1.09 (d, J = 7.8 Hz, 1H, $SiCH_2CH_2$), 1.22 (t, J = 7.1 Hz, 9H, $SiOCH_2CH_3$), 1.54 – 1.66 (m, 2H, $SiCH_2CH_2CH_2$), 3.38 (s, 3H, OCH_3), 3.41 (t, J = 7.2 Hz, 2H, $SiCH_2CH_2CH_2$), 3.52 – 3.69 (m, 12H, CH_2CH_2O) and 3.82 (q, J = 7.0 Hz, 6H, $SiOCH_2CH_3$).

PEO-silane amphiphile (n = 8): *1* (20.02 g, 15.57 mmol), allyl methyl PEO_8 (6.60 g, 15.57 mmol) and Karstedt's catalyst were reacted together.[44] In this way, the product (22.68 g, 85% yield) was obtained. ^{1}H NMR (δ, ppm): -0.02 – 0.14 (m, 90H, $SiCH_3$), 0.47 – 0.53 (m, 2H, $SiCH_2CH_2CH_2$), 0.55 (s, 3H, $SiCH_2CH_2$), 1.08 (d, J = 7.5 Hz, 1H, $SiCH_2CH_2$), 1.22 (t, J = 7.1 Hz, 9H, $SiOCH_2CH_3$), 1.52 – 1.66 (m, 2H, $SiCH_2CH_2CH_2$), 3.37 (s, 3H, OCH_3), 3.40 (t, J = 7.2 Hz, 2H, $SiCH_2CH_2CH_2$), 3.51 – 3.68 (m, 32H, CH_2CH_2O) and 3.81 (q, J = 7.0 Hz, 6H, $SiOCH_2CH_3$).

PEO-silane amphiphile (n = 16): *1* (17.98 g, 13.98 mmol), allyl methyl PEO_{16} (10.85 g, 13.98 mmol) and Karstedt's catalyst were reacted together.[44] In this way, the product (23.55 g, 82% yield) was obtained. ^{1}H NMR (δ, ppm): -0.01 – 0.15 (m, 90H, $SiCH_3$), 0.47 – 0.54 (m, 2H, $SiCH_2CH_2CH_2$), 0.55 (s, 3H, $SiCH_2CH_2$), 1.09 (d, J = 7.5 Hz, 1H, $SiCH_2CH_2$), 1.22 (t, J = 6.9 Hz, 9H, $SiOCH_2CH_3$), 1.52 – 1.66 (m, 2H, $SiCH_2CH_2CH_2$), 3.37 (s, 3H, OCH_3), 3.41 (t, J = 7.2 Hz, 2H, $SiCH_2CH_2CH_2$), 3.52 – 3.72 (m, 64H, CH_2CH_2O) and 3.82 (q, J = 6.9 Hz, 6H, $SiOCH_2CH_3$).

Synthesis of siloxane- and PEO-controls (*n* = 3, 8, and 16)—PEO-controls (i.e. no siloxane tethers) (Figure 1) were prepared as previously reported for *n* = 8 by the Karstedt's-catalyzed hydrosilylation of triethoxysilane and the designated allyl methyl PEO_n (1.1:1.0 molar ratio).[44]

PEO-control (n = 3): Triethoxysilane(5.43 g, 33.1 mmol), allyl methyl PEO_3 (6.14 g, 30.1 mmol) and Karstedt's catalyst were reacted together. In this way, the product (7.53 g, 65% yield) was obtained. ^{1}H NMR (δ, ppm): 0.57 – 0.65 (m, 2H, $SiCH_2CH_2CH_2$), 1.20 (t, J = 6.9 Hz, 9H, $SiOCH_2CH_3$), 1.62 – 1.74 (m, 2H, $SiCH_2CH_2CH_2$), 3.36 (s, 3H, OCH_3), 3.41 (t, J = 6.9 Hz, 2H, $SiCH_2CH_2CH_2$), 3.51 – 3.68 (m, 12H, CH_2CH_2O) and 3.80 (q, J = 7.1 Hz, 6H, $SiOCH_2CH_3$).

PEO-control (n = 8): Triethoxysilane(4.24 g, 25.8 mmol), allyl methyl PEO_8 (9.94 g, 23.4 mmol) and Karstedt's catalyst were reacted together.[44] In this way, the product (9.32 g, 68% yield) was obtained. ^{1}H NMR (δ, ppm): 0.57 – 0.64 (m, 2H, $SiCH_2CH_2CH_2$), 1.20 (t, J = 7.1 Hz, 9H, $SiOCH_2CH_3$), 1.62 – 1.74 (m, 2H, $SiCH_2CH_2CH_2$), 3.36 (s, 3H, OCH_3), 3.41 (t, J = 6.8 Hz, 2H, $SiCH_2CH_2CH_2$), 3.50 – 3.66 (m, 32H, CH_2CH_2O) and 3.79 (q, J = 7.0 Hz, 6H, $SiOCH_2CH_3$).

PEO-control (n = 16): Triethoxysilane(1.57 g, 9.57 mmol), allyl methyl PEO_{16} (6.74 g, 8.69 mmol) and Karstedt's catalyst were reacted together. In this way, the product (4.17 g, 50% yield) was obtained. ^{1}H NMR (δ, ppm): 0.57 – 0.65 (m, 2H, $SiCH_2CH_2CH_2$), 1.20 (t, J = 6.9 Hz, 9H, $SiOCH_2CH_3$), 1.62 – 1.74 (m, 2H, $SiCH_2CH_2CH_2$), 3.36 (s, 3H, OCH_3), 3.41 (t, J = 6.9 Hz, 2H, $SiCH_2CH_2CH_2$), 3.50 – 3.71 (m, 64H, CH_2CH_2O) and 3.80 (q, J = 7.0 Hz, 6H, $SiOCH_2CH_3$).

Synthesis of siloxane-control (1): ***1*** served as the siloxane-control and was prepared as noted above for the first step of the synthesis of the PEO-silane amphiphiles. VTEOS (3.53 g, 18.6 mmol) and α,ω-bis-(SiH)oligodimethylsiloxane (20.37 g, 18.6 mmol) were reacted together.[44] In this way, the product (23.65 g, 99% yield) was obtained ^{1}H NMR (δ, ppm): 0.003 – 0.177 (m, 84H, $SiCH_3$), 0.19 (d, J = 7.5 Hz, 6H, $OSi[CH_3]_2H$), 0.56 (s, 3H, $SiCH_2CH_2$), 1.09 (d, J = 7.5 Hz, 1H, $SiCH_2CH_2$), 1.23 (t, J = 7.1 Hz, 9H, $SiOCH_2CH_3$), 3.83 (q, J = 7.0 Hz, 6H, $SiOCH_2CH_3$) and 4.67 – 4.73 (m, 1H, SiH).

Coating preparation

Preparation of surface-grafted coatings on silicon wafers—Silicon wafers (1″ × 1″) were cleaned by sequentially sonicating in (10 min) and rinsing with acetone, repeating with DI water and then drying in a 120 °C oven overnight. Next, the surfaces of the wafers were oxidized by submerging in a 7:3 v/v concentrated H_2SO_4/30% H_2O_2 (Piranha) solution for 30 min (warning: Piranha solution must be handled with extreme caution), removed, rinsed thoroughly with DI water and dried under a stream of air. In a typical procedure, grafting solutions comprised of each of the PEO-silane amphiphiles, PEO-controls and the siloxane-control were prepared at a concentration of 0.012 M in isopropanol (IPA) (30 mL). Following the addition of 1 drop of DI water, the grafting solutions were mixed in sealed jars for 1 h on a shaker table. Next, an oxidized wafer was placed into a jar and remained on

a shaker table for 12 h. Afterwards, the wafers were removed, air dried, and cured under vacuum (36 mm Hg) at 150 °C for 12 h. To remove unbound chains, the wafers were sequentially soaked (1 h), sonicated (3 min) and rinsed with ethanol, the sequence repeated with DI water and then lastly dried under a stream of air.

Preparation of modified silicone coatings—Glass microscope slides were sequentially rinsed with dichloromethane (DCM) and acetone followed by drying in a 120 °C oven overnight. Casting solutions were prepared by combining 2.0 g MED-1137 silicone in 6 g (9 mL) hexane and mixing with a vortexer until a homogenous solution was obtained. The PEO-silane amphiphiles, PEO-controls and siloxane-control were each added to individual casting solutions at 0.05 mmol of silane per 1.0 g silicone and mixed thoroughly. Solutions were solvent-cast onto leveled glass microscope slides (1.5 mL per slide) and a polystyrene Petri dish cover placed on top of each so as to slow solvent evaporation and prevent bubble formation. The films were allowed to cure for one week at RT and immediately used for designated analyses.

Surface Characterization

XPS—Surface composition analysis of surface-grafted coatings on silicon wafers was performed with a KRATO AXIS Ultra Imaging X-ray Photoelectron Spectrometer with a monochromatized Mg K_α source and operating at a base pressure of $\sim 2\% \times 10^{-9}$ mbar. The area of analysis was 7 × 3 mm. Elemental atomic percent compositions were determined from three survey spectra sweeps performed from 0 to 1100 eV. High resolution (HR) analyses with a pass energy of 40 eV were performed with a take-off angle of 90°. HR scans (180 s sweeps) were performed at 526 to 536 eV for O 1s, 280 to 295 eV for C 1s, and 96 to 106 eV for Si 2p. Raw data was quantified and analyzed using XPS Peak Processing software.

Ellipsometry—The thickness of surface-grafted coatings on silicon wafers was measured via ellipsometry (Alpha-SE, J.A. Woollam) with an incident angle of 70° in the spectral range of 380-900 nm and in the high-precision mode (30 s data acquisition time). The average thickness of the oxide layer of an oxidized silicon wafer was determined at three regions of a wafer specimen (taken from a wafer designated for grafting with a particular composition) using a standard two-layer (silica-silicon) optical model included in the manufacturer's software. To measure the thickness of the grafted chains, the previously determined oxide layer thickness was utilized in a second optical model that included the third “Cauchy layer” (polymer-silica-silicon). The index of refraction (n) was set to 1.450 which is that of crystalline PEO.[47, 53] The average thickness (h) of the grafted layers was based on four individual wafers, each measured at three different regions.

Water contact angle analysis—Static contact angles (θ_{static}) of DI water droplets were measured at RT using a CAM-200 goniometer (KSV Instruments) equipped with an autodispenser, video camera, and drop-shape analysis software (Attension Theta). Following deposition, a 5 μL sessile drop of water was iteratively measured over a 2 min (surface-grafted wafers) and 3 min (silicone-based coatings) period. The reported θ_{static} values of the surface-grafted wafers were based on four individual wafers, each measured at three

different areas (12 measurements total). The θ_{static} for the silicone-based coatings was an average of three measurements from different areas of the same film surface.

Protein adsorption—Protein adsorption onto surface-grafted coatings was measured by QCM-D (Q-Sense E4). Silicon dioxide coated sensors (50 nm thickness; Q-Sense) were ultrasonically cleaned with acetone and DI water as described above for silicon wafers. Following exposure to oxygen plasma for 2 min (Harrick Plasma, PDC-001), the sensors were surface-grafted with the designated PEO-silane amphiphile, PEO-control or siloxane-control as described above for silicon wafers. Contact angle analysis was used to verify grafting. Grafted sensors were subjected to the following sequence: (1) 150 μL/min flow of PBS until the frequency and dissipation values remained constant for > 5 min, (2) 150 μL/min flow of 100 μg/mL HF in PBS for 20 min and (3) 150 μL/min flow of PBS for 5 min to remove loosely bound protein. The manufacturer's software was used to process the raw data and determine the mass of HF adsorbed to each sensor.

The adsorption of AF-546 HF onto silicone coatings was measured via fluorescence microscopy. A silicone isolator well (20 mm well diameter, 2 mm depth; McMaster-Carr) was pressed against silicone films thereby creating a seal which prevented leakage of solution from the well. Fibrinogen solution (100 μg/mL in PBS, 0.7 mL) was added to each well. (Note: Per manufacturer specifications, the AF-546 was first dissolved in 0.1 M $NaHCO_3$ to obtain a 1.5 mg/mL solution and was further diluted in PBS to obtain a final concentration of 0.1 mg/mL.) After 3 h at RT (protected from light), the solution was removed and 0.7 mL of fresh PBS was then added to each well and removed after 5 min. This process was repeated five times with fresh PBS and lastly one time with DI water. The samples were dried under a stream of air and protected from light until imaged. For each coating, an additional specimen was prepared and likewise rinsed with PBS and DI water, but without exposure to AF-546 (i.e. soaked 3 h in PBS) in order to correct for the background intensity.

A FV1000 (Olympus) laser scanning confocal microscope was used for quantification of protein adsorption onto all films. Imaging conditions, both in excitation and collection, were identical for all samples: objective (SPLSAPO 10× objective, NA 0.40), laser excitation type and intensity (HeNe 543 nm source), field of view and resolution (256 × 256 pixels, 317 × 317 micron field of view), depth (40 slices at 1 μm per slice), slice averaging, and collection (150 μm pinhole, 560 nm long-pass filter followed by a 560-660 nm band-pass filter, identical photomultiplier voltages/sensitivities). Data analysis was performed on the FV10-ASW v3.1 software suite (Olympus). Each surface was imaged in three locations and aggregate intensities computed. These were compared to three images obtained from the analogous surface that had similar treatment without protein exposure. Changes in intensity from exposure to protein were then obtained and compared, with errors reported as the standard deviation of three measurements.

Conclusions

While the exceptional protein resistance of PEO (e.g. conventional PEO-silanes) is well described, these observations have largely been made when PEO is grafted to a physically

stable substrate (e.g. silicon wafer). In this way, migration of the PEO to the surface-water interface (where protein and other biological adhesion occurs) is not required. However, when PEO is used to bulk-modify a silicone elastomer, rapid water-driven restructuring is essential in order to affect protein resistance. In this work, both surface-grafted silicon and bulk-modified silicones were prepared with PEO-silane amphiphiles comprised of a siloxane tether (m = 13) and a PEO segment of variable lengths (n = 3, 8, and 16) as well as the corresponding PEO-controls (i.e. no siloxane tether). Surface-grafted PEO-controls, due to their greater hydrophilicity, demonstrated superior resistance to fibrinogen versus the PEO-silane amphiphiles. However, when used to bulk-modify a silicone, PEO-controls produced surfaces that remained hydrophobic after 3 min of exposure to water. As a result, these surfaces exhibited poor resistance to protein adsorption. In contrast, PEO-silane amphiphiles (n = 8 and 16) demonstrated dramatic and rapid water-driven surface restructuring, becoming extremely hydrophilic after exposure to water for only 3 min. As a result, these surfaces displayed exceptionally high resistance to fibrinogen. While the PEO-silane amphiphile (n = 3) also exhibited water-driven restructuring, the achieved hydrophilicity and resistance to protein was diminished by its low PEO content. The enhanced potential of PEO-silane amphiphiles to migrate to the surface-water interface and reduce protein adsorption may be attributed to the hydrophobic nature as well as flexibility of the siloxane tether which allows movement of the tether and attached PEO segment through the silicone network. Furthermore, these results point to the limitations of predicting PEO's protein resistance using model substrates.

Supplementary Material

Refer to Web version on PubMed Central for supplementary material.

Acknowledgments

The authors thank the Texas Engineering and Experiment Station (TEES) for financial support of this research. M.A. Rufin gratefully acknowledges support from the NIH (3R01DK95101-02S1). J.A. Gruetzner thanks the Texas A&M University Research Opportunities Experience Fellowship. J.E. Raymond acknowledges support from the Welch Foundation (#A-0001) and the Office of Naval Research (N00014-14-1-0082). We also thank Professor Karen L. Wooley (Texas A&M University, Department of Chemistry) and the Laboratory for Synthetic-Biologic Interactions for use of the QCM-D.

References

1. Curtis, J.; Colas, A. Biomaterials Science: An Introduction to Materials in Medicine. 2nd. Ratner, BD.; Hoffman, AS.; Schoen, FJ.; Lemons, JE., editors. Vol. ch. 7.19. Academic Press; New York: 2004. p. 697
2. Van Dyke, ME.; Clarson, SJ.; Arshady, R. An Introduction to Polymeric Biomaterials. Arshady, R., editor. Citrus Books; London: 2003. p. 109
3. El-Zaim, HS.; Heggers, JP. Polymeric Biomaterials. 2nd. Dumitriu, S., editor. Vol. ch. 3. Marcel Dekker; New York: 2001. p. 79
4. Lejars M, Margaillan A, Bressy C. Chem Rev. 2012; 112:4347. [PubMed: 22578131]
5. Brash JL. Annals of the New York Academy of Sciences. 1977; 283:356.
6. Krishnan S, Weinman CJ, Ober CK. J Mater Chem. 2008; 18:3405.
7. Hanson, SR. Biomaterials Science: An Introduction to Materials in Medicine. 2nd. Ratner, BD.; Hoffman, AS.; Schoen, FJ.; Lemons, JE., editors. Vol. ch. 4.6. Academic Press; New York: 2004. p. 332

8. Raad II, Luna M, Khalil SAM, Costerton JW, Lam C, Bodey GP. JAMA - J Am Med Assoc. 1994; 271:1014.
9. Lloyd DA, Shanbhogue LKR, Doherty PJ, Sunderland D, Hart CA, Williams DF. J Pediatr Surg. 1993; 28:345. [PubMed: 8468644]
10. Hron P. Polym Int. 2003; 52:1531.
11. Abbasi F, Mirzadeh H, Katbab AA. Polym Int. 2001; 50:1279.
12. Bodas D, Khan-Malek C. Microelectron Eng. 2006; 83:1277.
13. Yao K, Huang XD, Huang XJ, Xu ZK. J Biomed Mater Res A. 2006; 78A:684. [PubMed: 16739174]
14. Zhang H, Annich GM, Miskulin J, Osterholzer K, Merz SI, Bartlett RH, Meyerhoff ME. Biomaterials. 2002; 23:1485. [PubMed: 11829445]
15. Morra M, Occhiello E, Garbassi F. Clinical Materials. 1993; 14:255.
16. Lee JH, Ju YM, Kim DM. Biomaterials. 2000; 21:683. [PubMed: 10711965]
17. Archambault JG, Brash JL. Colloids and Surfaces B: Biointerfaces. 2004; 39:9. [PubMed: 15542334]
18. Balakrishnan B, Kumar DS, Yoshida Y, Jayakrishnan A. Biomaterials. 2005; 26:3495. [PubMed: 15621239]
19. Banerjee I, Pangule RC, Kane RS. Adv Mater. 2011; 23:690. [PubMed: 20886559]
20. Lee JH, Lee HB, Andrade JD. Prog Polym Sci. 1995; 20:1043.
21. Jeon SI, Lee JH, Andrade JD, De Gennes PG. J Colloid Interface Sci. 1991; 142:149.
22. Jeon SI, Andrade JD. J Colloid Interface Sci. 1991; 142:159.
23. Knoll D, Hermans J. J Biol Chem. 1983; 258:5710. [PubMed: 6853541]
24. Harris, JM., editor. Poly(Ethylene Glycol) Chemistry: Biotechnical and Biomedical Applications. Plenum Press; New York: 1992.
25. Browning MB, Cereceres SN, Luong PT, Cosgriff-Hernandez EM. J Biomed Mater Res A. 201410.1002/jbm.a.35096
26. Prime KL, Whitesides GM. J Am Chem Soc. 1993; 115:10714.
27. Feldman K, Hähner G, Spencer ND, Harder P, Grunze M. J Am Chem Soc. 1999; 121:10134.
28. Pale-Grosdemange C, Simon ES, Prime KL, Whitesides GM. J Am Chem Soc. 1991; 113:12.
29. Zhang M, Desai T, Ferrari M. Biomaterials. 1998; 19:953. [PubMed: 9690837]
30. Zhang M, Ferrari M. Biomed Microdevices. 1998; 1:81.
31. Papra A, Gadegaard N, Larsen NB. Langmuir. 2001; 17:1457.
32. Lee SW, Laibinis PE. Biomaterials. 1998; 19:1669. [PubMed: 9840002]
33. Jo S, Park K. Biomaterials. 2000; 21:605. [PubMed: 10701461]
34. Yasuda H, Sharma AK, Yasuda T. J Polym Sci Pol Phys. 1981; 19:1285.
35. Owen MJ, Smith PJ. J Adhes Sci Technol. 1994; 8:1063.
36. Owen, MJ. Silicon-based Polymer Science: A Comprehensive Resource. Zeigler, JM.; Fearon, FWG., editors. Vol. ch. 40. American Chemical Society; Washington, D.C: 1990. p. 705
37. Owen, MJ. Siloxane Polymers. Clarson, SJ.; Semlyen, JA., editors. Vol. ch. 7. Prentice Hall; Englewood Cliffs: 1993. p. 309
38. Mark, JE. Silicon-Based Polymer Science: A Comprehensive Review. Zeigler, JM.; Fearon, FWG., editors. Vol. 224, ch. 2. American Chemical Society; Washington, D.C: 1990. p. 47
39. Lane, TH.; Burns, SA. Immunology of Silicones. Potter, M.; Rose, NR., editors. Springer; Berlin: 1996. p. 3
40. Chen H, Brook MA, Sheardown H. Biomaterials. 2004; 25:2273. [PubMed: 14741592]
41. Chen H, Brook MA, Chen Y, Sheardown H. J Biomat Sci - Polym E. 2005; 16:531.
42. Thompson, DB.; Fawcett, AS.; Brook, MA. Silicon Based Polymers. Ganachaud, F.; Boileau, S.; Boury, B., editors. Vol. ch. 3. Springer; 2008. p. 29
43. Chen H, Zhang Z, Chen Y, Brook MA, Sheardown H. Biomaterials. 2005; 26:2391. [PubMed: 15585242]

44. Murthy R, Cox CD, Hahn MS, Grunlan MA. Biomacromolecules. 2007; 8:3244. [PubMed: 17725363]
45. Hawkins ML, Faÿ F, Réhel K, Linossier I, Grunlan MA. Biofouling. 2014; 30:247. [PubMed: 24447301]
46. Hawkins ML, Rufin MA, Raymond JE, Grunlan MA. J Mater Chem B. 2014; 2:5689.
47. Murthy R, Shell CE, Grunlan MA. Biomaterials. 2009; 30:2433. [PubMed: 19232435]
48. Murthy R, Bailey BM, Valentin-Rodriguez C, Ivanisevic A, Grunlan MA. J Polym Sci Pol Chem. 2010; 48:4108.
49. Hawkins ML, Grunlan MA. J Mater Chem. 2012; 22:19540.
50. Moreau O, Portella C, Massicot F, Herry JM, Riquest AM. Surf Coat Technol. 2007; 201:5994.
51. Cole MA, Thissen H, Losie D, Voelcker NH. Surf Sci. 2007; 601:1716.
52. Sofia SJ, Premnath V, Merrill EW. Macromolecules. 1998; 31:5059. [PubMed: 9680446]
53. Unsworth LD, Tun Z, Sheardown H, Brash JL. J Colloid Interface Sci. 2005; 281:112. [PubMed: 15567386]
54. Feng W, Brash JL, Zhu S. Biomaterials. 2006; 27:847. [PubMed: 16099496]
55. Sharma S, Johnson RW, Desai TA. Appl Surf Sci. 2003; 206:218.
56. Zdyrko B, Klep V, Luzinov I. Langmuir. 2003; 19:10179.
57. Harder P, Grunze M, Dahint R, Whitesides GM, Laibinis PE. The Journal of Physical Chemistry B. 1998; 102:426.
58. Soong R, Macdonald PM. Biochimica et Biophysica Acta (BBA) - Biomembranes. 2007; 1768:1805. [PubMed: 17524353]
59. Allen C, Dos Santos N, Gallagher R, Chiu GNC, Shu Y, Li WM, Johnstone SA, Janoff AS, Mayer LD, Webb MS, Bally MB. Biosience Rep. 2002; 22:225.
60. Sangermano M, Bongiovanni R, Malucelli G, Priola A, Pollicino A, Recca A. J Appl Polym Sci. 2003; 89:1524.
61. Pitt WG, Park K, Cooper SL. J Colloid Interf Sci. 1986; 111:343.
62. Tang L, Eaton JW. J Exp Med. 1993; 178:2147. [PubMed: 8245787]
63. Tsai WB, Grunkemeier JM, Horbett TA. J Biomed Mater Res. 1999; 44:130. [PubMed: 10397913]
64. Wu Y, Simonovsky FI, Ratner BD, Horbett TA. J Biomed Mater Res A. 2005; 74A:722. [PubMed: 16037938]
65. Hu WJ, Eaton JW, Ugarova TP, Tang L. Blood. 2001; 98:1231. [PubMed: 11493475]
66. Wei Q, Becherer T, Angioletti-Uberti S, Dzubiella J, Wischke C, Neffe AT, Lendlein A, Ballauff M, Haag R. Angew Chem Int Edit. 2014; 53:8004.
67. Nonckreman CJ, Fleith S, Rouxhet PG, Dupont-Gillain CC. Colloid Surface B. 2010; 77:139.
68. Hemmersam AG, Foss M, Chevallier J, Besenbacher F. Colloid Surface B. 2005; 43:208.
69. Park K, Shim Hong S, Dewanjee Mrinal K, Eigler Neal L. J Biomat Sci - Polym E. 2000; 11:1121.
70. Luan Y, Li D, Wang Y, Liu X, Brash JL, Chen H. Langmuir. 2014; 30:1029. [PubMed: 24393063]
71. Tanaka M, Sawaguchi T, Sato Y, Yoshioka K, Niwa O. Tetrahedron Lett. 2009; 50:4092.
72. Lord MS, Stenzel MH, Simmons A, Milthorpe BK. Biomaterials. 2006; 27:1341. [PubMed: 16183113]
73. Tanaka M, Mochizuki A, Motomura T, Shimura K, Onishi M, Okahata Y. Colloid Surface A. 2001; 193:145.
74. Cooper MA, Singleton VT. J Mol Recognit. 2007; 20:154. [PubMed: 17582799]
75. Lu DR, Park K. J Colloid Interf Sci. 1991; 144:271.
76. Geelhood SJ, Horbett TA, Ward WK, Wood MD, Quinn MJ. J Biomed Mater Res Part B Appl Biomater. 2007; 81B:251. [PubMed: 17022059]
77. Hooper R, Lyons LJ, Mapes MK, Schumacher D, Moline DA, West R. Macromolecules. 2001; 34:931.
78. Chang Y, Kwon YC, Lee SC, Kim C. Macromolecules. 2000; 33:4496.

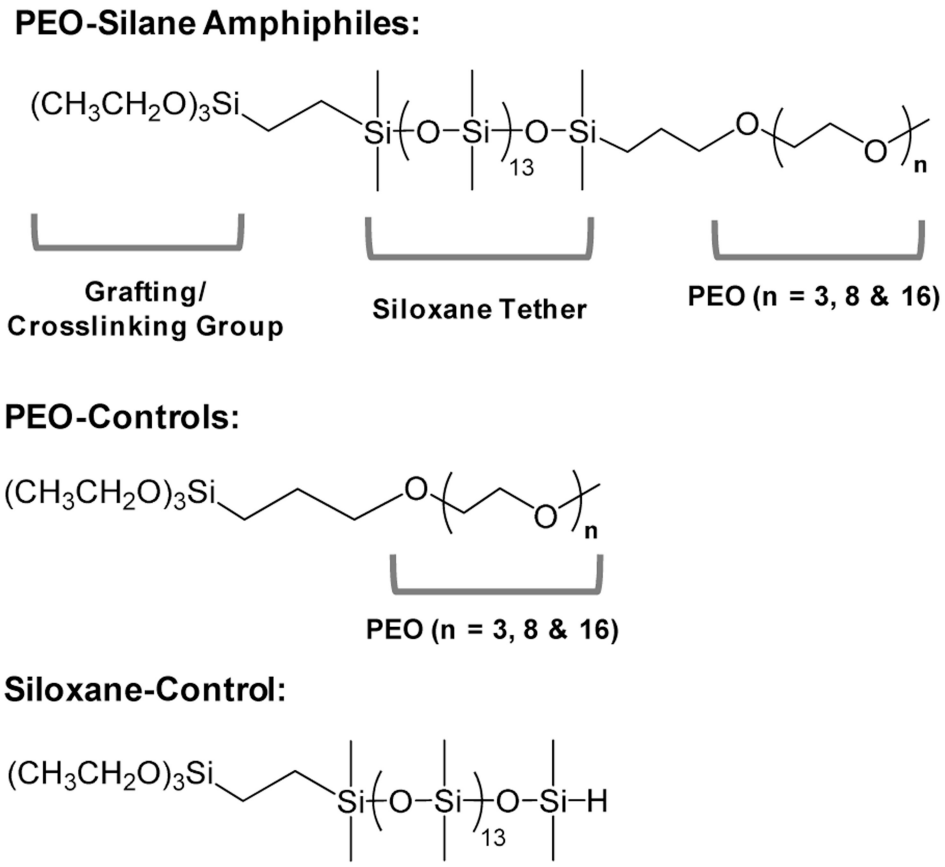

Figure 1.
Structures of PEO-silane amphiphiles, PEO-controls and siloxane-control.

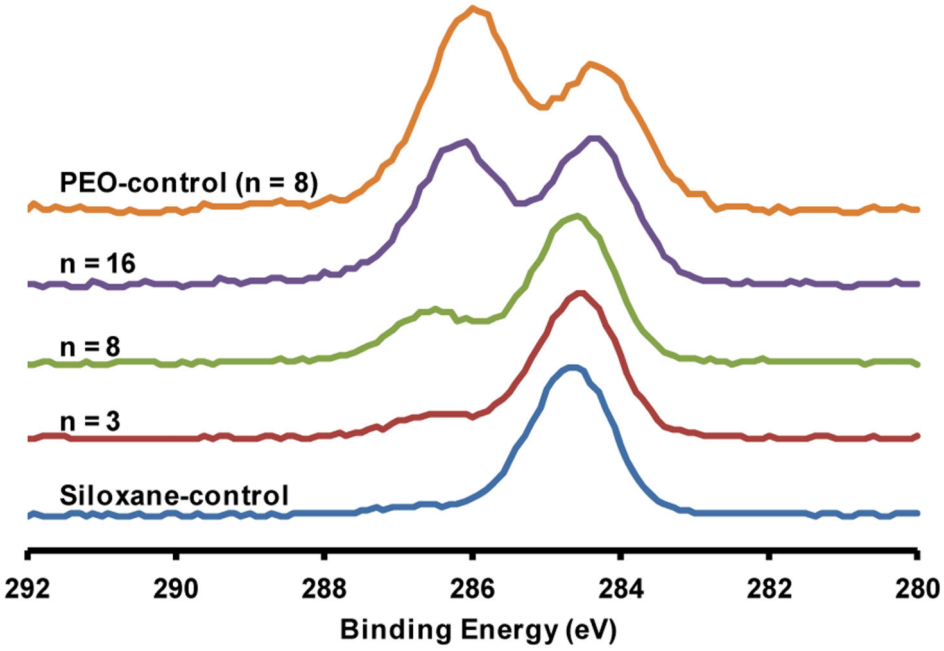

Figure 2.

HR C 1s XPS spectra of silicon wafers grafted with PEO-silane amphiphiles (n = 3, 8, and 16) as well as the PEO-control (n = 8) and siloxane-control.

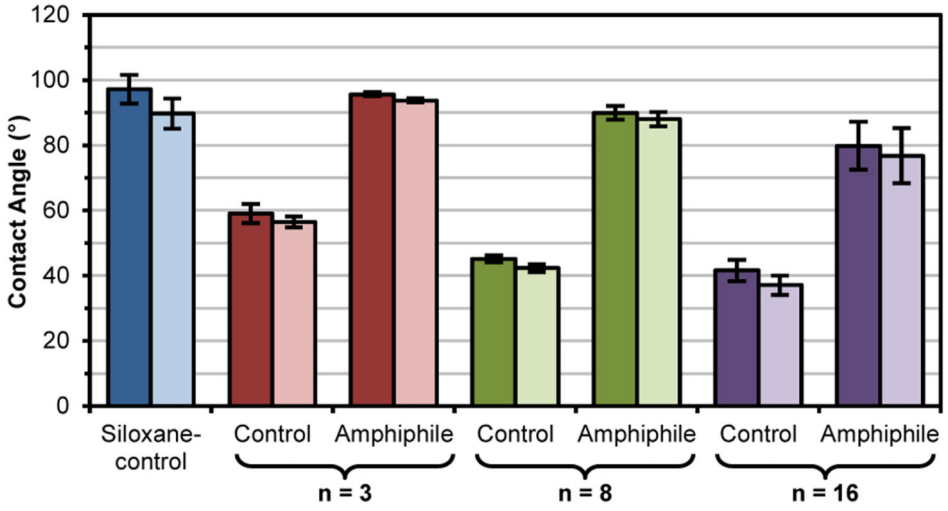

Figure 3.

Static contact angle (θ_{static}) of surface-grafted silicon wafers at 0 s (dark) and 2 min (light) following placement of water droplet. Each bar represents the average and standard deviation of measurements performed in triplicate on four identically prepared samples.

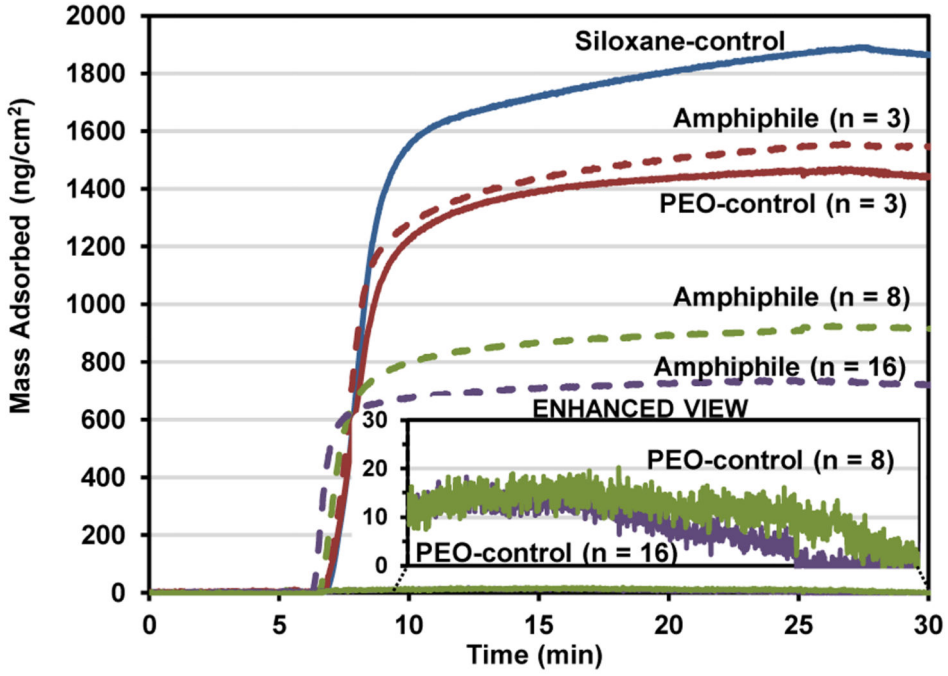

Figure 4.

QCM-D-measured adsorption of human fibrinogen (HF) onto silica-coated sensors grafted with the siloxane-control [blue solid line], PEO-silane amphiphiles (n = 3, 8, and 16) [dashed lines] and PEO-controls (n = 3, 8, and 16) [solid lines]. After equilibration for 5 min with PBS, the sensors were exposed to HF for 20 min and then to PBS for 5 min.

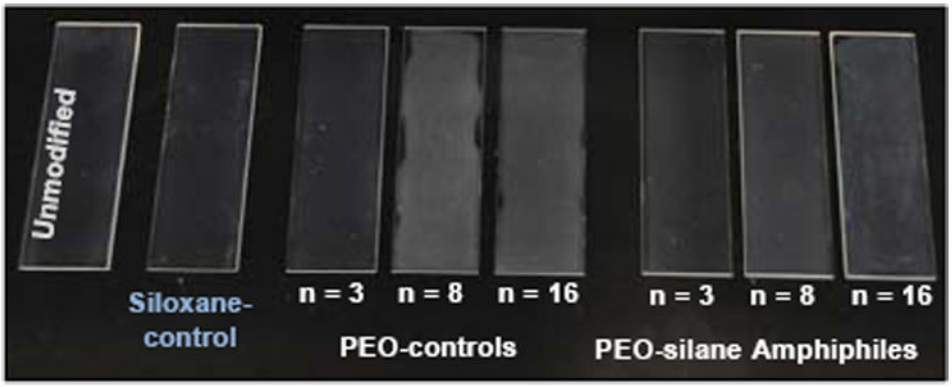

Figure 5.
Unmodified silicone and silicones bulk-modified with PEO-silane amphiphiles (n = 3, 8, and 16), PEO-controls (n = 3, 8, and 16) and the siloxane-control.

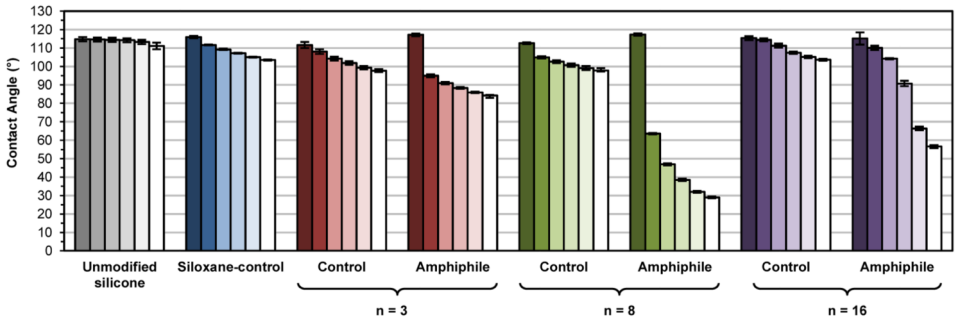

Figure 6.

Static water contact angles measured over three minutes on bulk-modified silicone films. Bars are organized as the time after initial drop placement from dark color to light as follows: 0 s, 15 s, 30 s, 1 min, 2 min and 3 min. Each bar represents the average of three contact angles measured at the same time point on the same sample and the error bar is the standard deviation.

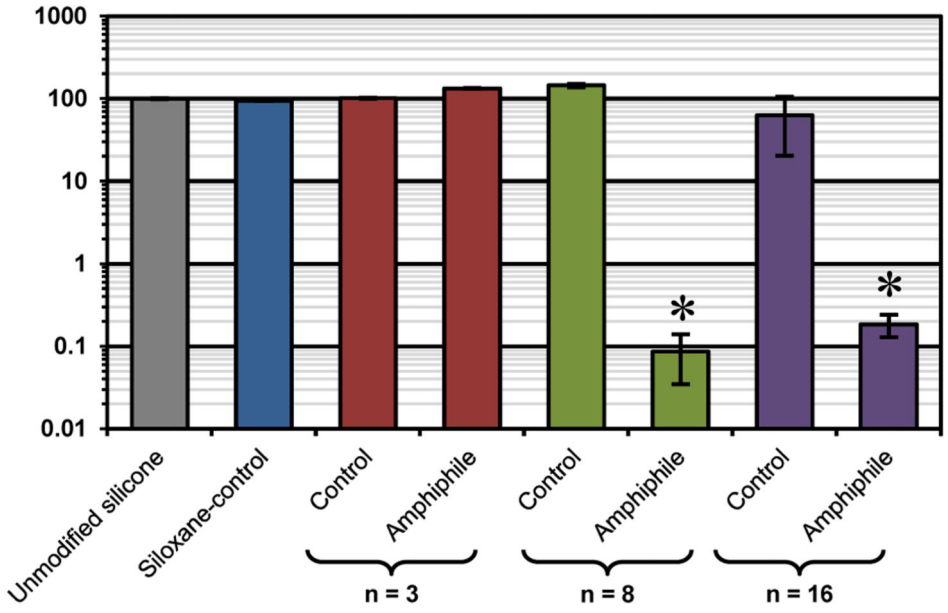

Figure 7.

Fibrinogen adsorption on bulk-modified silicones as measured by fluorescent intensity with confocal microscopy. Each bar represents the average and standard deviation of pixel intensity for three images normalized to unmodified silicone. Statistical significance was determined for low-fouling samples by one-way analysis of variance (Holm-Sidak method where * indicates $p < 0.05$).

Table 1

Surface atomic % composition by XPS.

	C 1s	*C-Si/C-C*	*C-O*	O 1s	Si 2p
Surface	**Total**	***284.5 eV***	***286.4 eV***		
Oxidized silica	**5**			**34**	**61**
Siloxane-control	**34**	94	6	**29**	**38**
n = 3	**24**	82	18	**29**	**47**
n = 8	**22**	71	29	**34**	**44**
n = 16	**26**	48	52	**33**	**42**
PEO-control (n = 8)	**26**	*38*	*62*	**35**	**38**

Table 2

Ellipsometry data for grafted surfaces.

Surface	M_n (g/mol)	Density ρ (g/mL)	Measured Thickness h (nm)	Chain Density $\sigma = (h\rho/M_n) \times N_A$ (chains/nm^2)	Chain Spacing $D = (4/\pi\sigma)^{1/2}$ (nm)	PEO Flory Spacing $2R_f = 2aN^{3/5}$ (nm)	Siloxane Flory Spacing $2R_f = 2aN^{1/3}$ (nm)
Siloxane-control	1286	1.01	2.5 ± 0.9	1.2 ± 0.4	**1.1 ± 0.2**	*n/a*	**2.4**
PEO-control (n = 3)	368	1.04	0.6 ± 0.1	1.0 ± 0.2	**1.1 ± 0.1**	**1.4**	*n/a*
PEO-control (n = 8)	588	1.13	2.3 ± 0.2	2.6 ± 0.2	**0.70 ± 0.03**	**2.4**	*n/a*
PEO-control (n = 16)	940	1.16	1.2 ± 0.2	0.9 ± 0.2	**1.2 ± 0.1**	**3.7**	*n/a*
Amphiphile (n = 3)	1490	1.04	2.1 ± 0.2	0.9 ± 0.1	**1.2 ± 0.1**	**1.4**	**2.4**
Amphiphile (n = 8)	1710	1.13	1.7 ± 0.2	0.6 ± 0.1	**1.4 ± 0.1**	**2.4**	**2.4**
Amphiphile (n = 16)	2062	1.04	3.1 ± 0.8	0.9 ± 0.2	**1.2 ± 0.1**	**3.7**	**2.4**